



Article

Flavopereirine—An Alkaloid Derived from *Geissospermum vellosii*—Presents Leishmanicidal Activity In Vitro

João Victor da Silva e Silva ^{1,2}, Helliton Patrick Cordovil Brigido ³,
Kelly Cristina Oliveira de Albuquerque ¹, Josiwander Miranda Carvalho ⁴,
Jordano Ferreira Reis ⁵ , Lara Vinhal Faria ⁵, Márlia Regina Coelho-Ferreira ⁶,
Fernando Tobias Silveira ⁷, Agnaldo da Silva Carneiro ⁵, Sandro Percário ^{8,9},
Andrey Moacir do Rosário Marinho ⁴ and Maria Fâni Dolabela ^{1,3,*} 

¹ Post-Graduate Program in Pharmaceutical Sciences, Federal University of Pará, Belém, PA 66075-110, Brazil; jvssilva89@gmail.com (J.V.d.S.e.S.); kellyoalbuquerque@hotmail.com (K.C.O.d.A.)

² Laboratory of Immunomodulation and Protozoology, Oswaldo Cruz Institute, FIOCRUZ, Rio de Janeiro, RJ 21040-900, Brazil

³ Post-Graduate Program in Pharmaceutical Innovation, Federal University of Pará, Belém, PA 66075-110, Brazil; helitom2009@hotmail.com

⁴ College of Chemistry, Federal University of Pará, Belém, PA 66075-110, Brazil; mcwander@hotmail.com (J.M.C.); andrey@ufpa.br (A.M.d.R.M.)

⁵ Faculty of Pharmacy, Federal University of Pará, Belém, PA 66075-110, Brazil; jordanoreis@outlook.com (J.F.R.); laravf24@gmail.com (L.V.F.); agsicar@yahoo.com.br (A.d.S.C.)

⁶ Emílio Goeldi Paraense Museum, Coordination of Botany, Ministry of Science, Technology, Innovation and Communications, Belém, PA 66077-530, Brazil; mcoelho@museu-goeldi.br

⁷ Evandro Chagas Institute, National Health Foundation, BR-316 Highway km 7, Ananindeua, PA 67030-000, Brazil; fernandotobias@iec.pa.gov.br

⁸ US Centers for Disease Control and Prevention (CDC), Atlanta, GA 30329, USA; percario@ufpa.br

⁹ Oxidative Stress Research Lab, Institute of Biological Sciences (ICB), Federal University of Pará, Belém, PA 66075-110, Brazil

* Correspondence: fanidolabela20@gmail.com; Tel.: +55-91-3201-8828

Academic Editors: Marcello Locatelli, Simone Carradori and Andrei Mocan

Received: 24 December 2018; Accepted: 27 January 2019; Published: 21 February 2019



Abstract: Chemotherapy is limited in the treatment of leishmaniasis due to the toxic effects of drugs, low efficacy of alternative treatments, and resistance of the parasite. This work assesses the in vitro activity of flavopereirine on promastigote cultures of *Leishmania amazonensis*. In addition, an in silico evaluation of the physicochemical characteristics of this alkaloid is performed. The extract and fractions were characterized by thin-layer chromatography and HPLC-DAD, yielding an alkaloid identified by NMR. The antileishmanial activity and cytotoxicity were assayed by cell viability test (MTT). The theoretical molecular properties were calculated on the Molinspiration website. The fractionation made it possible to isolate a beta-carboline alkaloid (flavopereirine) in the alkaloid fraction. Moreover, it led to obtaining a fraction with greater antileishmanial activity, since flavopereirine is very active. Regarding the exposure time, a greater inhibitory effect of flavopereirine was observed at 24 h and 72 h (IC₅₀ of 0.23 and 0.15 µg/mL, respectively). The extract, fractions, and flavopereirine presented low toxicity, with high selectivity for the alkaloid. Furthermore, flavopereirine showed no violation of Lipinski's rule of five, showing even better results than the known inhibitor of oligopeptidase B, antipain, with three violations. Flavopereirine also interacted with residue Tyr-499 of oligopeptidase B during the molecular dynamics simulations, giving a few insights of a possible favorable mechanism of interaction and a possible inhibitory pathway. Flavopereirine proved to be a promising molecule for its antileishmanial activity.

Keywords: leishmania; *Geissospermum vellosii*; apocynaceae; oligopeptidase B; flavopereirine; medicinal chemistry; in silico modeling

1. Introduction

Amazonian species belonging to the family Apocynaceae are characterized by the presence of alkaloids, many of which are used in traditional medicine in the treatment of hard-to-heal wounds [1]. Within this family, two genera have deserved special attention for possessing alkaloids that have been shown as promising antimalarial molecules: *Aspidosperma* and *Geissospermum*. However, there is a knowledge gap regarding the antileishmanial potential of these genera, with reports only describing the antileishmanial properties of *Aspidosperma ramiflorum* Muell. Arg. and *Geissospermum reticulatum* A. Gentry. The alkaloid extract of *A. ramiflorum* was active against promastigotes of *L. (L.) amazonensis* and *L. (V.) braziliensis* [2]. The extract was fractionated, isolating the alkaloids ramiflorines A and B. Both ramiflorines A and B showed activity against *Leishmania (L.) amazonensis* (LD₅₀ 16.3 ± 1.6 µg/mL and 4.9 ± 0.9 µg/mL, respectively) [3].

G. reticulatum presented in its composition the indole alkaloids *O*-demethylaspidospermine, which was active against *L. infantum* (IC₅₀ 7.7 µg/mL), with a smaller effect on *T. cruzi* (IC₅₀ 41.7 µg/mL); and *N*-Deacetyl-*N*-butanoylgeissospermidine, which was only active against *L. infantum* (IC₅₀ 52.2 µg/mL). When comparing the toxicity of these molecules against the reference drugs, amphotericin B and nifurtimox (CC₅₀ 10.3 and 13.9 µg/mL, respectively), the cytotoxicity of *O*-demethylaspidospermine was lower than both of them (CC₅₀ 16.7 µg/mL) when assayed using mammalian Chinese hamster ovaries (CHO). Therefore, *O*-demethylaspidospermine presented a better selectivity for *Leishmania* (Selectivity Index, SI = 2.17) [4].

Phytochemical studies of the species *Geissospermum vellosii* Allemão (Apocynaceae) led to the isolation of several compounds, shown in Figure 1. The alkaloids isolated from *G. vellosii* were tested in clones of *Plasmodium falciparum* chloroquine-sensitive strain, obtaining potential antiplasmodial results for the indole alkaloids geissolosimine (IC₅₀ 0.66 µg/mL), geissospermine (IC₅₀ 0.65 µg/mL), geissoschizoline (IC₅₀ 0.89 µg/mL), geissoschizone (IC₅₀ 1.78 µg/mL), and vellosiminol (IC₅₀ 1.04 µg/mL) [5]. Another study analyzed the activity against two strains of *P. falciparum* (chloroquine-resistant K1 and chloroquine-sensitive T9-96) with the indole alkaloids geissoschizoline and geissoschizoline N4-oxide presenting low selectivity (SI = 1; IC₅₀ and CC₅₀ > 40 µM). In addition, 1,2-dehydrogeissoschizoline showed a higher activity in the resistant clone (K1—CI₅₀ 27.26 µM; T9-96—CI₅₀ 35.37 µM), and the β-carboline alkaloid flavopereirine was more active in *P. falciparum* (K1—IC₅₀ 11.53 µM; T9-96—IC₅₀ 1.83 µM), with high selectivity for the sensitive parasite (SI = 5.85 for T9-96) [6]. Thus, among these alkaloids, flavopereirine was the most active tested compound. The antiplasmodial activity of *G. vellosii* was related to this alkaloid. However, no evaluation of the leishmanicidal activity for this alkaloid was found in the literature, and this evaluation was necessary.

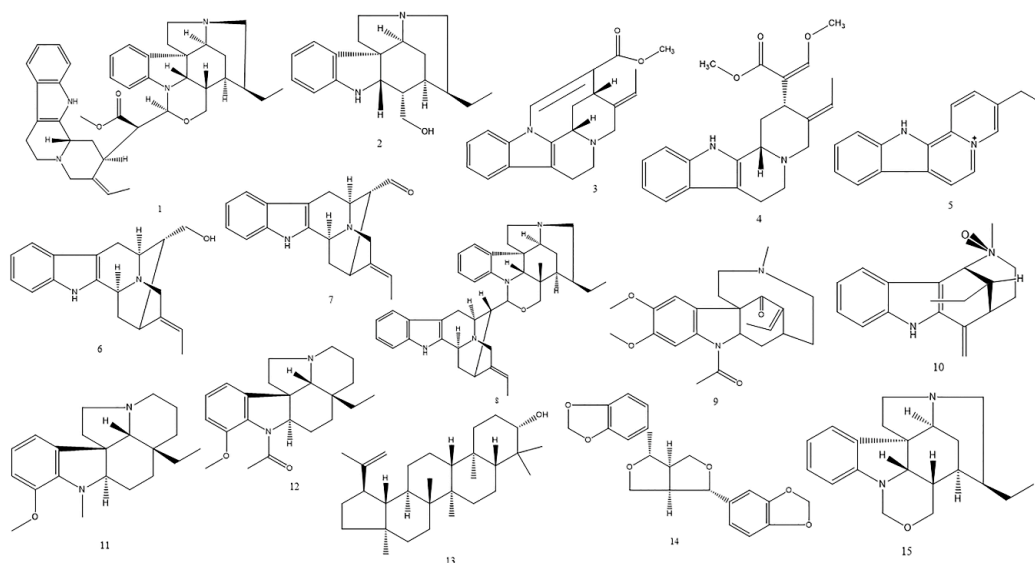


Figure 1. Main compounds isolated from *G. vellosii*. (1.1) Geissospermine [7]; (1.2) geissoschizoline; (1.3) apogeissoschizine; (1.4) geissoschizine [8]; (1.5) flavopereirine [9]; (1.6) vellosiminol; (1.7) vellosimine; (1.8) geissolosimine [10]; (1.9) geissovelline [11]; (1.10) pausperadine [12]; (1.11) 12-methoxy-1-methyl-aspidospermidine [13]; (1.12) aspidospermine; (1.13) lupeol; (1.14) sesamine [14]; (1.15) geissoschizone [5].

The physicochemical properties of certain functional groups are fundamental in the pharmacodynamic phase of the mechanisms of action of many drugs. This is because during the molecular recognition stage, the sum of the interacting forces of the pharmacophoric groups of the ligand with the complementary sites of the receptor is an essential factor for the pharmacological effect of the medicine. The pharmacokinetic phase of absorption, distribution, metabolization, and excretion is also a direct result of the bioavailability and half-life of a drug, being directly affected by the variation of physicochemical properties. Therefore, studies that associate *in silico* results with *in vitro* experiments will certainly contribute to help elucidate the main characteristics of a potential drug [15]. Moreover, studies have shown that oligopeptidase B (OpB)—a cytosolic protein belonging to the prolyl oligopeptidase family of serine proteases (Clan SC, family S9) [16,17], common in trypanosomatids [18]—regulates enolase levels on the cell surface of parasites of the genus *Leishmania*, which contributes to the virulence of several infectious agents. The connection between OpB and the parasite suggests that it is a key point in the host infection [19], being a promising target for the development of new antileishmanial drugs. Other studies have shown that alkaloids can significantly inhibit the activity of oligopeptidases [20–22]. However, the inhibitory activity of various alkaloids has not yet been evaluated. That being said, this work evaluates *in vitro* studies of flavopereirine on promastigote cultures of *Leishmania amazonensis* as well as the *in silico* properties of flavopereirine.

2. Results

2.1. *In Vitro* Results

2.1.1. *G. vellosii* Prospection and Phytochemical Profile Show the Presence of an Alkaloid

The ethanol extract obtained from barks of *G. vellosii* had a yield of 2.0% (Table 1). The extract was subjected to fractionation by extraction under reflux, resulting in four fractions. Of these, the methanol fraction showed the highest yield (85.2%; Table 1), indicating that the extract is rich in polar substances. Another method used for extract fractionation was the acid–base partition, yielding two fractions: neutral fraction (42.8%) and alkaloid fraction (27.5%; Table 1). This low yield of the alkaloid fraction suggests that the concentration of alkaloids in the extract is reduced.

Table 1. Yields and thin layer chromatography of *Geissospermum vellosii*.

Samples	Yield (%)	TLC	
		UV Light	Dragendorff
EE	2.0	+	+
NF	42.8	+	+
AF	27.5	+	+
FrHex	1.8	+	+
FrDcm	5.8	+	+
FrAcOET	2.2	+	+
FrMeOH	85.2	+	+

TLC, thin-layer chromatography; UV, ultraviolet rays; EE, Ethanol Extract; NF, Neutral Fraction; AF, Alkaloid Fraction; FrHex, Hexane Fraction; FrDcm, Dichloromethane Fraction; FrAcOET, Ethyl Acetate Fraction; FrMeOH, Methanol Fraction.

Thin-layer chromatography studies suggest that the extract and its fractions should have alkaloids (Table 1). The alkaloid fraction (AF) was subjected to chromatographic fractionation on a Sephadex LH-20 column, yielding subfraction F6AF. HPLC-DAD studies of subfraction F6AF suggested the presence of alkaloids, which led to the fractionation of that subfraction by preparative HPLC, giving the alkaloid flavopereirine (Figure 2).

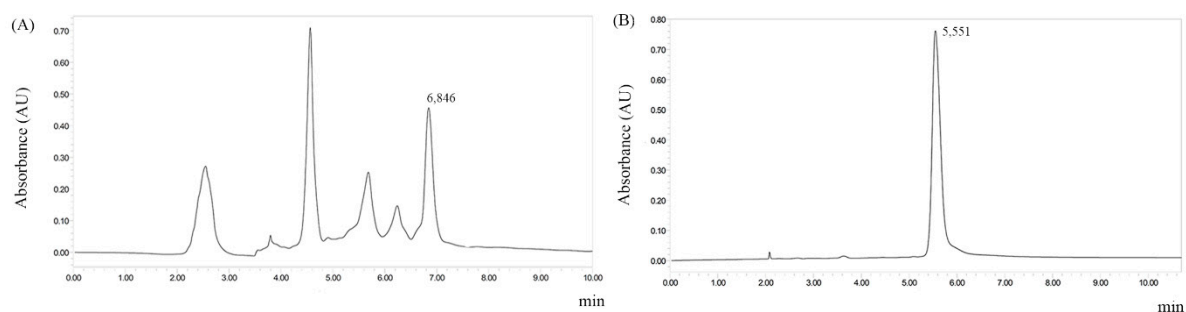


Figure 2. Chromatographic HPLC profiles of the subfraction F6AF and flavopereirine isolation of ethanolic extract from stem barks of *G. vellosii*. Condition: SunFire™ Prep. C18 OBD™ 5 μm 19 × 150 mm column, flow rate = 10.0 mL/min, temperature 18 °C. Mobile phase—t = 0 min: 80% water and 20% acetonitrile; t = 10 min: 80% water and 20% acetonitrile. (A) Chromatogram to subfraction F6AF; (B) flavopereirine-isolated *G. vellosii*.

2.1.2. The Alkaloid Derived from Flavopereirine Presents High Antipromastigote Activity

The antipromastigote activity of the extract, fractions, and alkaloid were evaluated at different times (24, 48, and 72 h). Most of the active samples showed better inhibitory effects at 24 h, and this effect was reduced at 48 h. The acid–base fractionation contributed to obtaining a very active fraction, the alkaloid fraction (AF). Further fractionation of this fraction yielded flavopereirine, which is probably the alkaloid responsible for such activity (Table 2).

The extract of *G. vellosii* underwent re-extraction under reflux. The hexane and ethyl acetate fractions were not promising as antileishmanial. Nevertheless, the methanol fraction was shown to be active, especially at 24 h. Fraction FrDcm also presented better activity at 24 h. However, the antipromastigote effect appears to be reduced with increased exposure time (Table 2).

Subfraction F6AF showed up to be more active than the alkaloid fraction itself (t = 24 h). Notwithstanding, at 72 h, no significant difference was observed between them ($p > 0.05$). Flavopereirine displayed pronounced antileishmanial activity at all times (Table 2).

Table 2. The anti-promastigote activity of *G. Vellosii*.

Samples	IC ₅₀ (µg/mL) + SD		
	24 h	48 h	72 h
EE	50.25 ± 0.36	29.57 ± 0.83	14.71 ± 0.70
FrHex	84.31 ± 0.50	>200	>200
FrDcm	5.56 ± 0.70	20.85 ± 0.25	10.06 ± 0.80
FrAcOET	12.32 ± 0.69	82.06 ± 0.26	88.61 ± 0.20
FrMeOH	1.71 ± 0.15	3.75 ± 0.52	5.95 ± 0.66
NF	34.59 ± 0.83	21.33 ± 0.19	18.25 ± 0.91
AF	6.22 ± 0.25	10.19 ± 0.18	1.07 ± 0.24
F6AF	1.56 ± 0.16 *	31.50 ± 0.76 *	1.24 ± 0.15 *
Flavopereirine	0.23 ± 0.10 * (0.93 µM)	2.34 ± 0.50 * 9.3 µM	0.15 ± 0.06 * 0.61 µM
Amphotericin	0.42 ± 0.09 (0.45 µM)	1.79 ± 0.06 (1.94 µM)	0.35 ± 0.01 (0.30 µM)

EE, Ethanol Extract; NF: Neutral Fraction; AF: Alkaloid Fraction; FrHex: Hexane Fraction; FrDcm: Dichloromethane Fraction; FrAcOET: Ethyl Acetate Fraction; FrMeOH: Methanol Fraction; * $p < 0.05$. **Legend:** The control of the untreated and solvent control presented viability corresponding to 100%.

2.1.3. Cytotoxicity and Selectivity Index of Flavopereirine Improved with Exposure Time in Comparison to Amphotericin B

Similar to the evaluation of antileishmanial activity, *G. vellosii* cytotoxicity was evaluated against modified THP-1 cells at different treatment times. A reduction of cytotoxicity with increased exposure time and no significant toxicity at 48 and 72 h of exposure ($CC_{50} > 400 \mu\text{g/mL}$) was observed. The extract, subfraction F6AF, flavopereirine, and amphotericin B proved to be very selective ($SI > 10$). When comparing the selectivity of flavopereirine over amphotericin B, it was observed that flavopereirine was more selective than amphotericin B, both at 24 h and 72 h (Table 3).

Table 3. Cytotoxicity (CC_{50}) and selective index (SI) of *G. Vellosii*.

Samples	24 h		48 h		72 h	
	CC ₅₀ *	SI	CC ₅₀ *	SI	CC ₅₀ *	SI
EE	178.0 ± 0.36	13.1	581.1 ± 0.60	19.7	829.4 ± 1.09	56.4
NF	115.9 ± 0.35	3.4	514.4 ± 0.61	23.4	744.3 ± 0.23	32.4
AF	121.4 ± 0.29	19.5	535.4 ± 0.43	52.5	774.3 ± 0.47	723.7
F6AF	443 ± 0.45	147.8	625.7 ± 0.34	19.9	629.4 ± 0.91	508.0
Flavopereirine	225.5 ± 0.9 (910 µM)	976.2	533.3 ± 0.15 (2156 µM)	228.2	734.0 ± 0.86 (2968 µM)	4993.2
Amphotericin	272.7 ± 0.09 (295.1 µM)	655.5	584.6 ± 0.46 (632.6 µM)	326.6	637.7 ± 0.72 (690 µM)	1811.7

* Human monocytic leukemia cell line (THP-1), concentration (µg/mL); EE, Ethanol Extract; NF, Neutral Fraction; AF, Alkaloid Fraction.

2.2. In Silico Results

2.2.1. Flavopereirine Presented Better Theoretical Properties than Antipain

To understand this effect of flavopereirine, in silico studies were performed. The compiled results from the theoretical properties of the Molinspiration website [23] are shown in Table 4. Flavopereirine showed a rather theoretical lipophilic LogP (0.90; Table 4), while antipain presented a hydrophilic profile (−3.01; Table 4). In addition, flavopereirine presented no violation of Lipinski's rule of five, which differs from antipain, with 3 violations (Table 4).

Table 4. Theoretical properties calculated from Molinspiration website of all tested molecules.

Molecules \ Properties	Antipain	Flavopereirine
tLogP	−3.01	0.90
TPSA	282.51	19.89
Molecular Weight	604.71	247.32
nON	16	2
nOHNH	13	1
nViolations	3	0
nRotB	19	1
Volume	563.14	233.44

tLogP, Theoretical Octanol-Water Partition Coefficient; TPSA, Total Polar Surface Area; nON, number of hydrogen bond acceptors; nOHNH, number of hydrogen bond donors; nViolations, number of violations of Lipinski's rule of five [24]; nRotB, number of rotatable bonds.

2.2.2. Flavopereirine Appears to Inhibit OpB by Directly Binding to Tyr-499 in Silico

Figure 2 shows that our docking method was enough to ideally represent how antipain acts by inhibiting OpB, showing a RMSD of 0.3601 Å. We analyzed the best-docked pose of antipain superposed with crystallographic antipain (Figure 3). In this sense, the chosen methodology showed to be adequate for the subsequent computational simulations of flavopereirine.

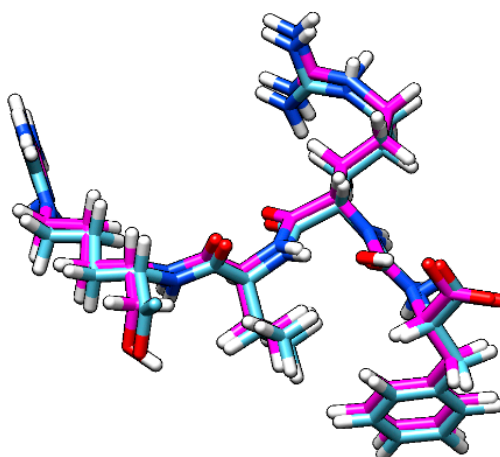


Figure 3. Docked antipain superposed with antipain from crystallography. In magenta, docked antipain; in blue, crystallographic antipain.

The bidimensional representation of our molecule docked in OpB is presented in Figure 3, showing the intermolecular interactions between both flavopereirine and OpB residues. It is possible to note that the hydrophobic interactions are the only ones present in the form of Van der Waals interactions (green outline) and π -stacking interactions (green dotted line) (Figure 4).

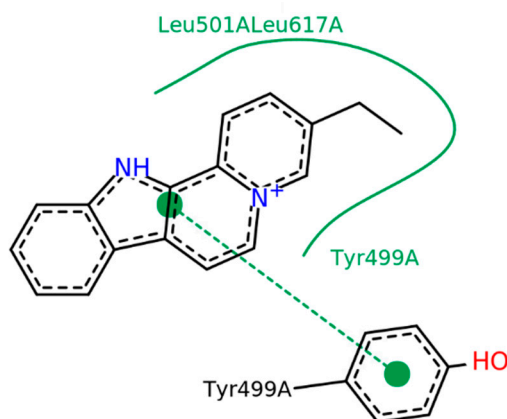


Figure 4. Intermolecular interactions between flavopereirine and OpB. In green outline, Van der Waals interactions; in dotted green line, π -stacking interactions. Image generated using PoseView (Version 1.1, BioSolveIT GmbH, St. Augustin, Germany) [25].

2.2.3. Flavopereirine Shows High Affinity to OpB in the Molecular Dynamics Simulation

The results of molecular dynamics are represented in Figure 5. Moreover, in Figure 5a, it is shown how the complex OpB-flavopereirine fluctuated through the molecular dynamics. Our results demonstrated that both OpB and flavopereirine fluctuated very little and stood in a very similar conformation to the structure at the beginning of the dynamics, having a RMSD lower than 2 Å. The free binding energy calculated by the MMPBSA method was -15.2747 kcal/mol. Figure 5b shows the individual contribution of each residue to the free binding energy.

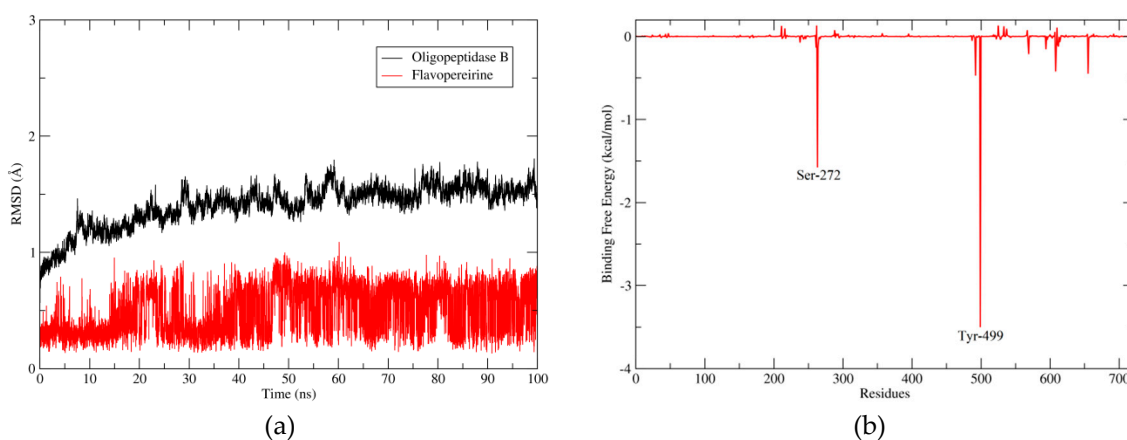


Figure 5. Molecular dynamics results. (a) RMSD x Time graphic of the molecular dynamics, with the black line representing the fluctuation of OpB and the red line the fluctuation of flavopereirine. (b) The main contributions to the binding free energy of each residue from OpB, mainly Ser-272 and Tyr-499.

A strong and attractive interaction between flavopereirine and residue Tyr-499, which is responsible for the abstract recognition of OpB, was computationally verified; this might be impeding the binding site and provoking the inactivation of this important enzyme of the parasite.

3. Discussion

The leishmanicidal activities of the alkaloid, extract, and fractions were evaluated after different exposure times. Flavopereirine and fractions containing the alkaloids (AF, F6AFGV, FDcm, and FMeOH) were very promising against promastigote forms of *L. amazonensis* ($IC_{50} < 10$ $\mu\text{g/mL}$), showing a rapid inhibitory effect on the parasite, as assessed after the first hours of exposure (Table 3). Extracts and fractions containing alkaloids were active against promastigote forms of *L. amazonensis*;

however, flavopereirine was the most active. This fact was also observed in the literature evaluating its antiplasmodial in vitro activity against two strains of *P. falciparum* (multidrug-resistant clone K1 and chloroquine-sensitive T9-96; K1-IC₅₀ 11.53 μ M and T9-96-IC₅₀ 1.83 μ M) [6]. A very positive point observed in this study was that bioguided fractionation made it possible to gain more information about secondary metabolites, which may contribute to the leishmanicidal activity as well as to the improvement of selectivity (Table 3). This suggests that flavopereirine is the pharmacological marker of the activity observed for that species. Furthermore, it is worth noting that this is the first report on the leishmanicidal effects of flavopereirine. This beta-carbolic alkaloid has been shown to be more selective than amphotericin B, a drug that presents a complexity of factors (e.g., toxicity) that make treatment compliance difficult. Therefore, the search for therapeutic alternatives with less toxicity for leishmaniasis is very important.

Oligopeptidase B (OpB) is a cytosolic protein belonging to the prolyl oligopeptidase family of serine proteases (Clan SC, family S9) [16,17]. It is a protein common in trypanosomatids [18], being involved in the cleavage of peptides in the carboxyl region of basic residues, with preference for arginine or lysine residues [26,27]. With the in vitro results in hand, it is very important to clarify the possible inhibitory mechanisms of action of flavopereirine using in silico approaches. To start, we chose *L. major* OpB as a target because of the known correlation between alkaloids and oligopeptidase inhibition [21,28] and because of the known similarities of prolyl oligopeptidase and OpB [29]. Lipinski's rule of five was initially applied to express the theoretical properties of flavopereirine and antipain, a potent inhibitor of OpB [30].

The compiled results from the theoretical properties demonstrated that flavopereirine did not present any violation of Lipinski's rule of five (Table 4), showing drug-like characteristics with respect to bioavailability. The results also show that flavopereirine is more lipophilic than antipain, implying a better capacity of trespassing membranes and acting intracellularly, which is essential for inhibiting OpB, a cytosolic enzyme [31]. It is also observed, through Total Polar Surface Area (TPSA) values, that flavopereirine (19.89) has a greater transport capacity in the biological environment when compared to antipain (282.51) [32]. Still, according to the theoretical studies performed, from the tested molecules, flavopereirine presented itself as the most drug-like molecule by having no violations to Lipinski's rule of five [33]. Lipinski has established that three or more violations of the rule could negatively impact the pharmacokinetics of any drug-aspiring molecule [24,33]. The incapability of antipain to cross membranes and its inhibitory effects on other peptidases and proteinases might be the reason for its non-use as a leishmanicidal agent.

The molecular docking results showed great interaction between flavopereirine and residue Tyr-499, an important residue for the abstract recognition of OpB [30]. The RMSD results from the molecular dynamics simulations showed a very stable binding to OpB, presented in Figure 5a with a graph lower than 1 Å throughout the entire simulation. Even though the ligand does not interact with any of the known residues of the canonical catalytic triad (Ser-577, His-697, Asp-662), this interaction with Tyr-499 might be strong enough to stabilize the complex [30]. Such interaction was emphasized according to the free binding energy results calculated using the Molecular Mechanics Poisson–Boltzmann/Surface Area (MM-PBSA) method. MM-PBSA is a simple but rather accurate end-state method of computing binding energy [34–38]. It showed a low energy, suggestive of a good interaction, which may be enough to prevent the OpB substrate to reach the catalytic site, and inhibiting the action of the enzyme.

4. Materials and Methods

4.1. Theoretical Molecular Properties

To calculate theoretical molecular properties, such as LogP, total polar surface area, number of hydrogen bond donors and acceptors, molecular weight, number of atoms, and number of rotatable bonds of flavopereirine, antipain, and amphotericin B, the Molinspiration website was used [23].

4.2. Molecular Docking

The tridimensional structure of oligopeptidase B (OpB) from *Leishmania major* was obtained from the Protein Data Bank (PDB), under the code 2XE4 [30]. Flavopereirine's tridimensional structure was downloaded from PubChem (PubChem ID: 65171) [39]. To perform the molecular docking, Molegro Virtual Docker (MVD) software version 4.3.0 (CLC Bio, Aarhus, Denmark) was used [40]. The binding cavity from the known inhibitor of OpB, antipain, was used as a reference to proceed with the simulation. The MolDock score function was selected with a grid resolution of 0.20 Å and an interaction radius of 12 Å. The search algorithm used was "MolDock SE". After performing 100 runs, there were 10 poses generated based on the interaction energy.

4.3. Molecular Dynamics Simulation

The best pose from the molecular docking was chosen as the starting conformation for the molecular dynamics studies. The electrostatic potentials (ESP) of flavopereirine were calculated at the Hartree–Fock level with the 6-31G* basis set, using Gaussian 09 (Gaussian, Inc., Wallingford, CT, USA) [41]. Flavopereirine was parametrized by assigning the restrained electrostatic potential (RESP) using the Antechamber and ParmEd.py modules of the AmberTools13 package [42]. All missing hydrogens were added using the TLEaP module [42]. Using the same module, TIP3P water molecules were added in an octahedral box of 8 Å surrounding the complex, and as many counterions were added as necessary [43].

Energy minimization and molecular dynamics simulations were performed using Amber 12 packages and PMEMD software (Version 12.0, University of California, San Francisco, CA, USA) [42]. All minimizations included a total of 5000 cycles. For the first 3000 cycles, we used the steepest-descent algorithm [44], and for the last 2000 cycles, we used the conjugate gradient algorithm [45]. During all minimization steps, a cut-off of 8 Å was defined for intermolecular interactions. After the minimization, the system was gradually heated from 0 to 300 K in six steps at 25 ps each, summing 150 ps and restricting the binding site. With the system heated properly, molecular dynamics was performed using general amber force field (gaff) [46] for flavopereirine, and ff12SB [47] for OpB, using sander and PMEMD modules from Amber12 software (University of California, San Francisco, CA, USA).

To evaluate the results of molecular dynamics, we used the root-mean-square deviation (RMSD) of atomic positions that represent the conformational differences and fluctuations of all molecules during the molecular dynamics, using the CPPTRAJ module from Amber12 [48]. The free binding energy was also calculated using the MM-PBSA method, and the energy was decomposed by residues to see which residues contributed more to the stability of the complex [36,37].

4.4. Plant Material

Stem barks were collected in a land area in the village of Ananin (12/13/2012), a municipality of Peixe-Boi, Pará State, Brazil (01°04'54.2" S, 47°18'58.6" W). The voucher specimen was deposited at the Herbarium of the Museu Paraense Emílio Goeldi under the record MG-Etn-00245.

4.5. Biological Material

The parasite used was *Leishmania (L.) amazonensis*, isolated from a human case from Ulianópolis, Pará State (MHOM/BR/2009/M26361). Cell lines from acute monocytic leukemia (THP-1; ATCC No. TIB 202) were purchased from the cell bank of Rio de Janeiro (BCRJ).

4.6. Phytochemical Studies

The powder from the barks underwent maceration with ethanol (1:10), and the macerated material was concentrated in a rotary evaporator until residue precipitation. The extract was then submitted to acid–base partition, yielding the neutral fraction (NF) and the alkaloid fraction (AF). The AF was subjected to further fractionation in the chromatography column using Sephadex LH-20 as

the stationary phase. Subfraction F6AF was subjected to fractionation in high-performance liquid chromatography (column SunFire™ Prep. C18 OBD™, 5 µm; 19 × 150 mm, Waters Corporation, Milford, MA, USA), resulting in the isolation of flavopereirine. For identification of this alkaloid, the Alliance HPLC-DAD system Waters (column SunFire™ C18 5 µm; 4.6 × 150 mm), LC-MS (WATERS® ACQUITY TQD SYSTEM/ESI using 50 mm × 2.1 mm 1.7µm Acquity UPLC BEH® C18 analytical column, Waters Corporation, Milford, MA, USA), and NMR Varian Mercury 300 (300 MHz, CD₃OD, Varian, Oxford, UK) were used.

The ethanolic extract was subjected to extraction under reflux [49], yielding 4 fractions: hexane, dichloromethane, ethyl acetate, and methanol. The extract and its fractions were subjected to characterization in thin-layer chromatography (Silicycle, Quebec City, QC, Canada) (TLC; revelators: UV and Dragendorff's reagent) and high-performance liquid chromatography with diode-array detection (HPLC-DAD, Manufacturer, Milford, MA, USA).

Flavopereirine: data from UV: λ 234.3, 288.8, 346.1, 385.4 nm; data from MS: [M + H]⁺ m/z 315.37, 297.65, 160.21, 122.27; NMR ¹H (300 MHz, CD₃OD): 8.76 (d, 9.0), 8.30 (d, 8.1), 9.16 (s), 8.87 (d, 6.3), 8.66 (d, 6.9), 8.36 (d, 7.8), 7.48 (t, 7.8), 7.74 (t, 6.9), 7.82 (d, 8.4), 2.99 (q, 7.5), 1.45 (t, 7.2).

4.7. Antipromastigote Assay

Field isolates of *Leishmania amazonensis* (MHOM/BR/2009/M26361) were obtained from the Instituto Evandro Chagas, Brazil. Promastigotes of *L. amazonensis* were isolated on NNN (Novy-Nicolle-Mcneal) blood slopes. Afterwards, the strains were subcultured and adapted to RPMI 1640 medium supplemented with 10% heat inactivated fetal bovine serum (Gibco®, Grand Island, NY, USA) and cultivated at 26 °C [50].

The logarithmic phase of growth of promastigote forms was adjusted to 5 × 10⁶ parasites/100 µL. The susceptibility assay was performed on 96-well plates. The extract, fraction, and alkaloids were assayed in triplicates on a concentration gradient (200–3.125 µg/mL). The negative control was assessed with only parasites and the incubation medium; the positive control was assayed with amphotericin B (25–0.3906 µg/mL). After 24 h, 48 h, and 72 h of incubation at 26 °C under 5% CO₂ atmosphere, 10 µL of the tetrazolium salt ([3-(4,5-dimethylthiazol-2-yl)-2,5-diphenyltetrazolium bromide], 5 mg/mL) was added to each well, and the parasites were quantified in the enzyme-linked immunosorbent assay plate reader [50]. The IC₅₀ was determined by linear regression (Graph Pad Prism version 6.01, GraphPad Software, San Diego, CA, USA).

4.8. Cell Viability Assay

Cell viability was determined by the MTT assay ([3-(4,5-dimethylthiazol-2-yl)-2,5-diphenyltetrazolium bromide]) [51]. THP-1 modified cells (4 × 10⁵ cells/0.1 mL) were grown in RPMI-1640 medium (Sigma Aldrich®, St Louis, MO, USA), supplemented with 5% fetal bovine serum, and kept under 5% CO₂ atmosphere at 37 °C. The cells were treated with extracts, fractions, subfractions, and alkaloids in different concentrations (ranging from 7.8125 to 500 µg/mL). After 24 h, 48 h, and 72 h of further incubation, MTT (5.0 mg/mL) was added. The plate was incubated at 37 °C in an atmosphere of 5% CO₂ for 4 h. Dimethyl sulfoxide was added to each well to solubilize formazan crystals. Optical density was determined at 490 nm (Stat Fax 2100 microplate reader, Awareness Technology, Inc, Palm City, FL, USA). Cell viability was expressed as a percentage of the control absorbance in the untreated cells after subtracting the appropriate background. Cytotoxic concentration (CC₅₀) was determined by linear regression [52].

5. Conclusions

In summary, our results suggest that *Geissospermum vellosii*, especially its indole alkaloid, flavopereirine, was very promising against *Leishmania amazonensis*. Moreover, its IC₅₀ is lower than that obtained for amphotericin B, the last-resort drug for leishmaniosis treatment. That may be related to its interaction with OpB, presented in the docking results and maintained throughout the entirety

of the molecular dynamics via π -stacking intermolecular interaction, presenting a possible novel inhibitory mechanism never shown before, and it may prevent substrates reaching the catalytic site.

Author Contributions: J.V.d.S.e.S. and M.F.D. designed the study, wrote the paper, and participated in the research; H.P.C.B., K.C.O.d.A., and L.V.F. participated in the research; J.M.C. and A.M.d.R.M. took part in alkaloids content determination using layer chromatography and HPLC-DAD and RMN; J.F.R. and A.d.S.C. performed and analyzed the *in silico* studies; M.R.C.-F. carried out the collection and identification of botanical material; S.P. contributed to the analysis of the data. All authors discussed the data obtained and collaborated in drafting the manuscript.

Funding: This research was funded by the National Council for Scientific and Technological Development [CNPq; Scholarship DT 310608/2013-9 Universal; 483894/2012-5] and PROPESP/UFPA (www.propesp.ufpa.br).

Acknowledgments: The authors thank all the collaborators of the UFPA's Pharmacology and Neglected Diseases laboratories, Emílio Goeldi Paraense Museum and Evandro Chagas Institute for technical support.

Conflicts of Interest: The authors declare no conflict of interest.

References

1. Vásquez, S.P.F. Conhecimento, uso e conservação da diversidade vegetal em quatro comunidades ribeirinhas no município Manacapuru, Amazonas. *Instituto Nacional de Pesquisas da Amazônia* **2014**, *xiv*, 87f.
2. Ferreira, I.C.P.; Lonardon, M.V.C.; Machado, G.M.C.; Leon, L.L.; Filho, L.G.; Pinto, L.H.B.; De Oliveira, A.J.B. Anti-leishmanial activity of alkaloidal extract from *Aspidosperma ramiflorum*. *Mem. Inst. Oswaldo Cruz* **2004**, *99*, 325–327. [[CrossRef](#)] [[PubMed](#)]
3. Tanaka, J.C.A.; da Silva, C.C.; Ferreira, I.C.P.; Machado, G.M.C.; Leon, L.L.; de Oliveira, A.J.B. Antileishmanial activity of indole alkaloids from *Aspidosperma ramiflorum*. *Phytomedicine* **2007**, *14*, 377–380. [[CrossRef](#)] [[PubMed](#)]
4. Reina, M.; Ruiz-Mesia, W.; López-Rodríguez, M.; Ruiz-Mesia, L.; González-Coloma, A.; Martínez-Díaz, R. Indole alkaloids from *Geissospermum reticulatum*. *J. Nat. Prod.* **2012**, *75*, 928–934. [[CrossRef](#)] [[PubMed](#)]
5. Mbeunkui, F.; Grace, M.H.; Lategan, C.; Smith, P.J.; Raskin, I.; Lila, M.A. *In vitro* antiplasmodial activity of indole alkaloids from the stem bark of *Geissospermum vellosii*. *J. Ethnopharmacol.* **2012**, *139*, 471–477. [[CrossRef](#)] [[PubMed](#)]
6. Steele, J.C.P.; Veitch, N.C.; Kite, G.C.; Simmonds, M.S.J.; Warhurst, D.C. Indole and β -carboline alkaloids from *Geissospermum sericeum*. *J. Nat. Prod.* **2002**, *65*, 85–88. [[CrossRef](#)] [[PubMed](#)]
7. Marion, L. Chapter XIII The Indole alkaloids. In *Alkaloids: Chemistry and Physiology*; Manske, R.H.F., Holmes, H.L., Eds.; Academic Press: New York, NY, USA, 1952; Volume 2, pp. 369–498.
8. Rapoport, H.; Onak, T.P.; Hughes, N.A.; Reinecke, M.G. Alkaloids of *Geissospermum vellosii*. *J. Am. Chem. Soc.* **1958**, *80*, 1601–1604. [[CrossRef](#)]
9. Hughes, N.; Rapoport, H. Flavopereirine, an alkaloids from *Geissospermum vellosii*. *J. Am. Chem.* **1958**, *80*, 1604–1609. [[CrossRef](#)]
10. Rapoport, H.; Moore, R.E. Alkaloids of *Geissospermum vellosii*. Isolation and structure determinations of Velloimine, Velloiminol, and Geissosimine. *J. Org. Chem.* **1962**, *27*, 2981–2985. [[CrossRef](#)]
11. Moore, R.E.; Rapoport, H. Geissoveline, a new alkaloid from *Geissospermum vellosii*. *J. Org. Chem.* **1973**, *38*, 215–230. [[CrossRef](#)]
12. Ishiyama, H.; Matsumoto, M.; Sekiguchi, M.; Shigemori, H.; Ohsaki, A.; Kobayashi, J. Two new indole alkaloids from *Aspidosperma subincanum* and *Geissospermum vellosii*. *Heterocycles* **2005**, *66*, 651–658. [[CrossRef](#)]
13. Werner, J.A.T.; Oliveira, S.M.; Martins, D.F.; Mazzardo, L.; de Fátima Gaspari Dias, J.; Lordello, A.L.L.; Miguel, O.G.; Royes, L.F.; Ferreira, J.; Santos, A.R.S. Evidence for a role of 5-HT_{1A} receptor on antinociceptive action from *Geissospermum vellosii*. *J. Ethnopharmacol.* **2009**, *125*, 163–169. [[CrossRef](#)] [[PubMed](#)]
14. Dias, J.D.F.G. Fitoquímica e ensaios biológicos do extrato bruto etanólico, frações e substâncias isoladas provenientes das cascas de *Geissospermum Vellosii* ALLEMÃO (Apocynaceae), Universidade Federal do Paraná. 2012. Available online: <https://acervodigital.ufpr.br/handle/1884/28287?show=full> (accessed on 26 September 2018).

15. Andrade, E.L.; Bento, A.F.; Cavalli, J.; Oliveira, S.K.; Freitas, C.S.; Marcon, R.; Schwanke, R.C.; Siqueira, J.M.; Calixto, J.B. Non-clinical studies required for new drug development—Part I: Early in silico and in vitro studies, new target discovery and validation, proof of principles and robustness of animal studies. *Br. J. Med. Biol. Res.* **2016**, *49*, e5644. [[CrossRef](#)] [[PubMed](#)]
16. Barrett, A.J.; Rawlings, N.D. Families and clans of serine peptidases. *Arch. Biochem. Biophys.* **1995**, *318*, 247–250. [[CrossRef](#)] [[PubMed](#)]
17. Rawlings, N.D.; Barrett, A.J. MEROPS: The peptidase database. *Nucleic Acids Res.* **1999**, *27*, 325–331. [[CrossRef](#)] [[PubMed](#)]
18. Morty, R.E.; Lonsdale-Eccles, J.D.; Mentele, R.; Auerswald, E.A.; Coetzer, T.H.T. Trypanosome-derived oligopeptidase B is released into the plasma of infected rodents, where it persists and retains full catalytic activity. *Infect. Immun.* **2001**, *69*, 2757–2761. [[CrossRef](#)] [[PubMed](#)]
19. Swenerton, R.K.; Zhang, S.; Sajid, M.; Medzihradzsky, K.F.; Craik, C.S.; Kelly, B.L.; McKerrow, J.H. The oligopeptidase B of *Leishmania* regulates parasite enolase and immune evasion. *J. Biol. Chem.* **2011**, *286*, 429–440. [[CrossRef](#)] [[PubMed](#)]
20. Cahlíková, L.; Hrabínová, M.; Kulhánková, A.; Benešová, N.; Chlebeka, J.; Jun, D.; Novák, Z.; Macáková, K.; Kuneš, J.; Kuča, K.; et al. Alkaloids from *Chlidanthus fragrans* and their Acetylcholinesterase, Butyrylcholinesterase and Prolyl Oligopeptidase Activities. *Nat. Prod. Commun.* **2013**, *8*, 1541–1544. [[PubMed](#)]
21. Cahlíková, L.; Hulová, L.; Hrabínová, M.; Chlebek, J.; Hošťálková, A.; Adamcová, M.; Šafratová, M.; Jun, D.; Opletal, L.; Ločárek, M.; et al. Isoquinoline alkaloids as prolyl oligopeptidase inhibitors. *Fitoterapia* **2015**, *103*, 192–196. [[CrossRef](#)] [[PubMed](#)]
22. Šafratová, M.; Hostalková, A.; Hulcová, D.; Breiterová, K.; Hrabcová, V.; Machado, M.; Fontinha, D.; Prudêncio, M.; Kuneš, J.; Chlebek, J.; et al. Alkaloids from *Narcissus poeticus* cv. Pink Parasol of various structural types and their biological activity. *Arch. Pharm. Res.* **2018**, *41*, 208–218. [[CrossRef](#)] [[PubMed](#)]
23. Molinspiration. Available online: <http://www.molinspiration.com/cgi-bin/properties> (accessed on 3 October 2018).
24. Lipinski, C.A. Lead- and drug-like compounds: The rule-of-five revolution. *Drug Discov. Today Technol.* **2004**, *1*, 337–341. [[CrossRef](#)] [[PubMed](#)]
25. Stierand, K.; Maaß, P.C.; Rarey, M. Molecular complexes at a glance: Automated generation of two-dimensional complex diagrams. *Bioinformatics* **2006**, *22*, 1710–1716. [[CrossRef](#)] [[PubMed](#)]
26. Rea, D.; Hazell, C.; Andrews, N.W.; Morty, R.E.; Fülöp, V. Expression, purification and preliminary crystallographic analysis of oligopeptidase B from *Trypanosoma brucei*. *Acta Crystallogr. Sect. F Struct. Biol. Cryst. Commun.* **2006**, *62*, 808–810. [[CrossRef](#)] [[PubMed](#)]
27. Coetzer, T.H.T.; Goldring, J.P.D.; Huson, L.E.J. Oligopeptidase B: A processing peptidase involved in pathogenesis. *Biochimie* **2008**, *90*, 336–344. [[CrossRef](#)] [[PubMed](#)]
28. Siatka, T.; Adamcová, M.; Opletal, L.; Cahlíková, L.; Jun, D.; Hrabínová, M.; Kuneš, J.; Chlebek, J. Cholinesterase and prolyl oligopeptidase inhibitory activities of alkaloids from argemone platyceras (*Papaveraceae*). *Molecules* **2017**, *22*, 1181. [[CrossRef](#)] [[PubMed](#)]
29. Oligopeptidase B—An overview. ScienceDirect Topics. Available online: <https://www.sciencedirect.com/topics/biochemistry-genetics-and-molecular-biology/oligopeptidase-b> (accessed on 5 November 2018).
30. McLuskey, K.; Paterson, N.G.; Bland, N.D.; Isaacs, N.W.; Mottram, J.C. Crystal structure of *Leishmania major* oligopeptidase B gives insight into the enzymatic properties of a trypanosomatid virulence factor. *J. Biol. Chem.* **2010**, *285*, 39249–39259. [[CrossRef](#)] [[PubMed](#)]
31. Munday, J.C.; McLuskey, K.; Brown, E.; Coombs, G.H.; Mottram, J.C. Oligopeptidase B deficient mutants of *Leishmania major*. *Mol. Biochem. Parasitol.* **2011**, *175*, 49–57. [[CrossRef](#)]
32. Pajouhesh, H.; Lenz, G.R. Medicinal chemical properties of successful central nervous system drugs. *NeuroRx* **2005**, *2*, 541–553. [[CrossRef](#)]
33. Lipinski, C.A.; Lombardo, F.; Dominy, B.W.; Feeney, P.J. Experimental and computational approaches to estimate solubility and permeability in drug discovery and development settings. *Adv. Drug Deliv. Rev.* **1997**, *64*, 3–25. [[CrossRef](#)]
34. Kollman, P.A.; Massova, I.; Reyes, C.; Kuhn, B.; Huo, S.; Chong, L.; Lee, M.; Lee, T.; Duan, Y.; Wang, W.; et al. Calculating structures and free energies of complex molecules: Combining molecular mechanics and continuum models. *Accounts Chem. Res.* **2000**, *33*, 889–897. [[CrossRef](#)]

35. Homeyer, N.; Gohlke, H. Free energy calculations by the molecular mechanics poisson-boltzmann surface area method. *Mol. Inform.* **2012**, *31*, 114–122. [[CrossRef](#)] [[PubMed](#)]
36. Miller, B.R.; McGee, T.D.; Swails, J.M.; Homeyer, N.; Gohlke, H.; Roitberg, A.E. MMPBSA.py: An efficient program for end-state free energy calculations. *J. Chem. Theory Comput.* **2012**, *8*, 3314–3321. [[CrossRef](#)] [[PubMed](#)]
37. Genheden, S.; Ryde, U. The MM/PBSA and MM/GBSA methods to estimate ligand-binding affinities. *Expert Opin. Drug Discov.* **2015**, *10*, 449–461. [[CrossRef](#)] [[PubMed](#)]
38. Su, P.C.; Tsai, C.C.; Mehboob, S.; Hevener, K.E.; Johnson, M.E. Comparison of radii sets, entropy, QM methods, and sampling on MM-PBSA, MM-GBSA, and QM/MM-GBSA ligand binding energies of *F. tularensis* enoyl-ACP reductase (FabI). *J. Comput. Chem.* **2015**, *36*, 1859–1873. [[CrossRef](#)] [[PubMed](#)]
39. PubChem Compound Database CID=65171. Available online: <https://pubchem.ncbi.nlm.nih.gov/compound/65171> (accessed on 1 April 2018).
40. Thomsen, R.; Christensen, M.H. MolDock: A new technique for high-accuracy molecular docking. *J. Med. Chem.* **2006**, *49*, 3315–3321. [[CrossRef](#)] [[PubMed](#)]
41. Frisch, M.J.; Trucks, G.W.; Schlegel, H.B.; Scuseria, G.E.; Robb, M.A.; Cheeseman, J.R.; Scalmani, G.; Barone, V.; Mennucci, B.; Petersson, G.A.; et al. *Gaussian 09*; Gaussian, Inc.: Wallingford, CT, USA, 2009.
42. Case, D.A.; Darden, T.A.; Cheatham III, T.E.; Simmerling, C.L.; Wang, J.; Duke, R.E.; Luo, R.; Walker, R.C.; Zhang, W.; Merz, K.M.; et al. *Amber 12*; University of California: San Francisco, CA, USA, 2012.
43. Joung, I.S.; Cheatham, T.E. Determination of alkali and halide monovalent ion parameters for use in explicitly solvated biomolecular simulations. *J. Phys. Chem. B* **2008**, *112*, 9020–9041. [[CrossRef](#)] [[PubMed](#)]
44. Courant, R. Variational methods for the solution of problems of equilibrium and vibrations. *Bull. Am. Math. Soc.* **1943**, *49*, 1–24. [[CrossRef](#)]
45. Fletcher, R. Function minimization by conjugate gradients. *Comput. J.* **1964**, *7*, 149–154. [[CrossRef](#)]
46. Wang, J.; Wolf, R.M.; Caldwell, J.W.; Kollman, P.A.; Case, D.A. Development and testing of a general Amber force field. *J. Comput. Chem.* **2004**, *25*, 1157–1174. [[CrossRef](#)]
47. Perez, A.; MacCallum, J.L.; Brini, E.; Simmerling, C.; Dill, K.A. Grid-based backbone correction to the ff12SB protein force field for implicit-solvent simulations. *J. Chem. Theory Comput.* **2015**, *11*, 4770–4779. [[CrossRef](#)]
48. Roe, D.R.; Cheatham, T.E. PTRAJ and CPPTRAJ: Software for processing and analysis of molecular dynamics trajectory data. *J. Chem. Theory Comput.* **2013**, *9*, 3084–3095. [[CrossRef](#)] [[PubMed](#)]
49. Vale, V.V.; Vilhena, T.C.; Trindade, R.C.S.; Ferreira, M.R.C.; Percário, S.; Soares, L.F.; Pereira, W.L.A.; Brandão, G.C.; Oliveira, A.B.; Dolabela, M.F.; et al. Anti-malarial activity and toxicity assessment of *Himatanthus articulatus*, a plant used to treat malaria in the Brazilian Amazon. *Malar. J.* **2015**, *14*. [[CrossRef](#)] [[PubMed](#)]
50. Mota, E.F.; Rosario, D.M.; Silva Veiga, A.S.; Brasil, D.D.S.B.; Silveira, F.T.; Dolabela, M.F. Biological activities of *Croton palanostigma* Klotzsch. *Pharmacogn. Mag.* **2016**, *12*, 96. [[CrossRef](#)]
51. Mosmann, T. Rapid colorimetric assay for cellular growth and survival: Application to proliferation and cytotoxicity assays. *J. Immunol. Methods* **1983**, *65*, 55–63. [[CrossRef](#)]
52. Ngure, P.K.; Tonui, W.K.; Ingonga, J.; Mutai, C.; Ng, Z.; Rukungu, G.; Kimutai, A. In vitro antileishmanial activity of extracts of *Warburgia ugandensis* (Canellaceae), a Kenyan medicinal plant. *J. Med. Plants Res.* **2009**, *3*, 61–66. [[CrossRef](#)]

Sample Availability: Samples of the compound flavopereirine are available from the authors upon requesting.



© 2019 by the authors. Licensee MDPI, Basel, Switzerland. This article is an open access article distributed under the terms and conditions of the Creative Commons Attribution (CC BY) license (<http://creativecommons.org/licenses/by/4.0/>).